PERGAMON

Available online at www.sciencedirect.com

SCIENCE @ DIRECT®

Automatica 39 (2003) 1157–1169

automatica

www.elsevier.com/locate/automatica

Individual cylinder characteristic estimation for a spark injection engine☆

L. Benvenuti[a], M.D. Di Benedetto[b], S. Di Gennaro[b,*], A. Sangiovanni-Vincentelli[c,d]

[a] *Dipartimento di Informatica e Sistemistica "Antonio Ruberti", Università degli Studi di Roma "La Sapienza" Via Eudossiana 18, Rome 00184, Italy*
[b] *Dipartimento di lngegneria Elettrica, Via San Pantaleo 66, Rome 00186, Italy*
[c] *P.A.R.A.D.E.S., Università di L'Aquila, Poggio di Roio, L'Aquila 67040, Italy*
[d] *EECS Department, University of California at Berkeley, CA 94720, USA*

Received 24 January 2002; received in revised form 25 September 2002; accepted 19 February 2003

Abstract

Engine control policies are mostly based on the assumption that all injectors have the same behavior independent of location and aging. In reality, injectors do vary and age. To contain variations around a nominal value, tight tolerances are imposed on the manufacturing process. Even if the manufacturing process is tightly controlled, the air-to-fuel (A/F) ratio needed to satisfy emission constraints is difficult to achieve due to aging and even slight mismatch among different injectors. To devise control policies that take into account behavior differences among injectors, we need to estimate injector characteristics from measurements that are taken on the engine during its life time. In this paper, we present an estimation technique for injector characteristics based on a set of measurements that can be carried out using the sensors present in the car, i.e., intake manifold pressure, crank-shaft speed, throttle-valve plate angle, injection timings and exhaust A/F ratio, which is measured by a single UEGO sensor placed at the exhaust pipe output.

Keywords: Automotive; Injector; Recalibration; UEGO Sensor

1. Introduction

Today a great deal of emphasis is placed by automotive engineers on the development of closed-loop engine control systems that meet exhaust emission standards while minimizing fuel consumption and maximizing driving performance. Meeting emission constraints imply that the air-to-fuel (A/F) ratio of the mix provided to the combustion process by the injection system must be as close as possible to stoichiometric, which corresponds to the amount of air theoretically required to oxidize all the injected fuel.

Since the air flow is regulated by the throttle valve, controlled by the driver with the accelerator pedal, the control variable becomes the fuel flow provided by the injectors to the intake manifold. Regulating the fuel flow requires accurate estimation of the characteristics of the injectors.

It is in fact known that injector variability may cause cylinder-to-cylinder differences in the mixture composition of the order of 5% (Heywood, 1989). Cylinder-to-cylinder air–fuel maldistribution results in emission concentration imbalance between cylinders. These individual emission differences will not necessarily average out to produce an overall result equivalent to that obtained with all cylinders operating at the same A/F ratio. This is due to the nonlinear variation of hydrocarbons, nitrogen oxides and carbon monoxide concentrations with A/F ratio (Bush, Adams, Dua, & Markyvech, 1994; Heywood, 1989). Moreover, even in the case of perfectly matched injectors, cylinder-to-cylinder air–fuel maldistribution can arise from different individual cylinder behavior in breathing due to intake manifold structure and valve characteristics.

To reduce the air–fuel maldistribution due to injector characteristics imbalance, injectors are usually required to have close tolerances, up to 1%, resulting in high cost per

☆ This paper was not presented at any IFAC meeting. This paper was recommended for publication in revised form by Associate Editor Brett Ninness under the direction of Editor Torsten Söderstrom.

* Corresponding author.
E-mail addresses: benve@dis.uniroma1.it, lucab@parades.rm.cnr.it (L. Benvenuti), dibenede@ing.univaq.it (M.D. Di Benedetto), digennar@ing.univaq.it (S. Di Gennaro), alberto@eecs.berkeley.edu, alberto@parades.rm.cnr.it (A. Sangiovanni-Vincentelli).

0005-1098/03/$ - see front matter © 2003 Elsevier Science Ltd. All rights reserved.
doi:10.1016/S0005-1098(03)00077-3

injector. Injectors are in fact machined to tolerances of the order of 6% and then their tolerance is reduced to 2% (in the operation nominal range, i.e. when the on-time is greater than 500 μs) by a quite expensive off-line tuning process. Better tolerance can be achieved by an even more expensive process that consists of testing and appropriately grouping the injectors in the so-called matched injector sets.

To achieve accuracy in controlling the emission concentrations, control policies that can discern the contribution of each injector and thus overcome the cylinder-to-cylinder A/F imbalance, have been recently proposed (Bush et al., 1994; Grizzle, Dobbins, & Cook, 1991; Moraal, Cook, & Grizzle, 1993). These policies allow the accommodation of greater injector tolerances and consequently the reduction of the cost per injector. These are inherently closed-loop strategies, since they allow the tuning of the individual cylinder A/F using the signal of the exhaust-gas-oxygen (UEGO) sensor. In Grizzle et al. (1991), a single switching UEGO sensor is used for this purpose, while in Moraal et al. (1993) the estimation of the individual cylinder A/F is obtained from a model inversion of an eight-cylinder engine. A slight different approach is presented in Moraal et al. (1993), where the individual cylinder A/F is estimated at low engine speed for a six-cylinder engine, using two UEGO sensors. The drawback of these control strategies is that they are effective only under steady-state operating conditions. Therefore, in situations where the UEGO sensor signal is not reliable (transients and cold start conditions), they cannot be applied and different open-loop strategies have to be designed.

The open-loop strategies are based on the estimation/measurement of the air charged in each cylinder. Clearly, in this situation, the individual cylinder A/F can be successfully controlled only if the individual injector characteristics are known. This paper addresses this problem, providing the estimation of the individual injector characteristics, along with the individual air flow estimation. More in detail, we propose a method for the estimation of each injector's characteristics via measurements of the intake-manifold pressure, the crank-shaft speed, the throttle-valve plate angle, the injections on-time and the UEGO sensor reading from the exhaust. The estimation processes is carried out during steady-state conditions, and the resulting parameters can be stored and used in the open-loop strategies during the transients and the UEGO sensor warm up.

The estimation algorithm is based on a fairly accurate modelling of the cylinder air-filling process, of the exhaust manifold dynamics, and of the UEGO sensor. For the cylinder air-filling process, a standard lumped model is used (Grizzle, Cook, & Milam, 1994). To obtain an accurate estimation algorithm, we studied the dependence of the air charge dynamics on some characterizing variables (pressure sensor error, throttle offset area, off-line estimation volumetric efficiency error). For the exhaust manifold dynamics, the transport delays and the mixing between the air–fuel charges associated with the cylinders were considered. Finally, we considered a linear UEGO sensor modelled as a first-order lag plus a delay, a common assumption in the literature (e.g., Chang, Fekete, Amstutz, & Powell, 1995; Grizzle et al., 1991; Jones, Ault, Franklin, & Powell, 1995; Powell, Wu, & Aquino, 1981).[1] The idea behind the proposed approach is to estimate first the sensor error and the throttle offset area on the basis of steady pressure measurements, and then, to calculate the average air flow entering each cylinder using these estimations. Using information from a single linear UEGO sensor, the A/F ratio for each cylinder is estimated and the injector characteristics are obtained. In this last step, the UEGO sensor signal is appropriately sampled in order to invert the exhaust manifold and sensor dynamics to reconstruct the individual cylinder A/F's.

The paper is organized as follows. In Section 2, we formulate the estimation problem. In Section 3, we show how to estimate the average air-mass flow entering the cylinders (Benvenuti, Di Benedetto, Rossi, & Sangiovanni-Vincentelli, 1998). In Section 4, estimation of the F/A ratios is covered. In Section 5, we estimate the injector characteristics and in Section 6, we offer realistic simulations and concluding remarks.

2. Estimation strategy

In this section, we state our solution approach for the individual injector characteristic estimation problem for a spark ignition (SI) engine.

We are interested in obtaining the characteristics of the individual injector because the variables available for the engine control are the injection profile, i.e., approximately the time in which the injector is open, and the timing of the spark. The injection profile is used to control the fuel-mass flow into the cylinders that determines the behavior of the engine with respect to pollution, fuel consumption and driveability. The fuel mass per injection pulse can be assumed to be an affine function of the fuel injector on-time

$$\dot{m}_{\mathrm{f},i} = \frac{n}{30}\, g_i(T_i - T_{i,\mathrm{off}}), \qquad i = 1,\ldots,n_\mathrm{c}$$

where T_i is the time the injector is open (s), g_i the gain (kg/s) and $T_{i,\mathrm{off}}$ the offset (s) of each injector. Hence, the problem is to estimate g_i and $T_{i,\mathrm{off}}$. In Section 5, we show that these two parameters can be estimated once the fuel-mass flow $\dot{m}_{\mathrm{f},i}$ injected in *each* cylinder is estimated. The key measurement for determining $\dot{m}_{\mathrm{f},i}$ is the F/A ratio given by a *single* UEGO sensor. The UEGO sensor is capable of measuring the F/A ratio $\gamma(t)$. If indeed there were no mixing of the exhaust gases from the various cylinders in the exhaust manifold, the problem would be fairly simple. The complications arise from the partial overlap of the exhaust gases from each cylinder.

[1] The use of higher-order models for the A/F sensor does not change the core of our approach, since the effect of a more complex model is felt only in the computation of the inverse of the model.

Let

$$\gamma_i(t) = \frac{\dot{m}_{f,i}(t)}{\dot{m}_{a,i}(t)}, \quad i = 1,\dots,n_c \tag{1}$$

denote the F/A ratio released by the ith cylinder during the exhaust phase, where $\dot{m}_{a,i}(t)$ is the air-mass flow entering in each cylinder during the intake process, and n_c the number of cylinders. Note that the contribution to cylinder-to-cylinder air–fuel maldistribution of the different cylinder breathing characteristics is negligible with respect to the injectors' variability. Then, we assume that the average air-mass flow $\dot{m}_{a,i}$ entering each cylinder is the same. Therefore, if we could estimate ratio (1) and the air-mass flow $\dot{m}_{a,i}$, we could obtain the fuel flows $\dot{m}_{f,i}(t)$. The estimation of $\gamma_i(t)$ from the UEGO sensor measurement is the subject of Section 4 and is based on the inversion of

$$\gamma(t) = \varphi(\gamma_1(t),\dots,\gamma_{n_c}(t))$$

a function that will be derived considering that $\gamma(t)$ depends on the F/A ratio $\gamma_c(t)$ at the runner confluence, which, in turns, is a known function $f(\gamma_1(t),\dots,\gamma_{n_c}(t))$ of the F/A ratios.

The estimation process for the air-mass flow $\dot{m}_{a,i}$ is described in Section 3. $\dot{m}_{a,i}$ is a dynamical function of p_{man}, the mean value manifold pressure, and the volumetric efficiency, η_v. If we assume that

(H) the mean value intake manifold pressure p_{man} and the crankshaft speed n remain constant [2] then, $\dot{p}_{man} = 0$ and the average air-mass flow $\dot{m}_a = n_c \dot{m}_{a,i}$, entering the n_c cylinders, is equal to the average air-mass flow $\dot{m}_{a,th}$ passing through the throttle. The average air-mass flow is a function of the throttle-plate angle α, which is directly measurable, and of the throttle-offset area A^0_{th}, an unknown value slowly varying because of aging. We can measure the manifold pressure with an unknown error ε_p, and the volumetric efficiency with an unknown constant error ε_{η_v}. Hence, the estimation algorithm for $\dot{m}_{a,i}$ is based on the estimation of ε_p, ε_{η_v}, and A^0_{th}.

3. Air-mass flow estimation

In this section, we show how to estimate the average air-mass flow $\dot{m}_a$ entering the cylinders (Benvenuti et al., 1998). We have already observed (see the appendix for a summary of the derivation of these relationships) that we need first to estimate the mean value intake manifold pressure p_{man}, from measurements (A.3), and the volumetric efficiency η_v, given by (A.6). Since we can measure p_{man} with an unknown error ε_p, and we can estimate η_v with an unknown constant error ε_{η_v}, the problem is to determine estimations of these errors.

We suppose that the steady-state hypothesis (H) holds true, so that $\dot{p}_{man} = 0$ and the average air flow $\dot{m}_a$, given by (A.5), is equal to the average air flow $\dot{m}_{a,th}$ passing through the throttle, given by (A.2). Since this last quantity is a function of the throttle offset area A^0_{th}, an unknown value slowly varying because of aging, we need to estimate this parameter as well.

The proposed algorithm allows for estimating the errors ε_p, ε_{η_v} and the parameter A^0_{th} on the basis of three different steady-state measurements. We assume that the variables and parameters of the system remain unchanged during the three measurements. We assume also to measure the manifold pressure with an unknown error $\varepsilon_p \in [-3\%, 3\%]$, to estimate the volumetric efficiency η_v with an unknown constant error $\varepsilon_{\eta_v} \in [-10\%, 10\%]$ and to have an unknown offset area $A^0_{th} \in [0, 5]\ \mathrm{mm}^2$ for the throttle. Finally, we assume to have a F/A feedback control system which regulates the injection pulse duration T_i in such a way that the A/F ratio is close to stoichiometry.

Section 3.1 is devoted to the determination of estimates for ε_p, ε_{η_v} and A^0_{th}, while in Section 3.2 we will determine the average air flow $\dot{m}_a$.

3.1. Sensor-error and throttle-offset area estimations

Two cases are considered: the case in which the ambient pressure is known and the one when it is unknown.

3.1.1. The case of known ambient pressure

From hypothesis (H), $\dot{p}_{man} = 0$ so that $\dot{m}_{a,th} = \dot{m}_a$. Then, using (A.2) and (A.5), we obtain

$$A_{e,th}(\alpha) + A^0_{th} = \frac{V_d n p_{man}}{120 p_{atm}\sqrt{RT_{atm}}} \frac{\eta_v(n, p_{man})}{\beta(p_{man}/p_{atm})},$$

where expression (A.4) for $A_{th}(\alpha)$ has been used. Substituting p_{man} obtained from (A.3), and using (A.6) for η_v, we have

$$\begin{aligned}&(A_{e,th}(\alpha) + A^0_{th})(1+\varepsilon_p)\\ &\quad = (1+\varepsilon_{\eta_v})\eta_v^{est}(n, p_m, \varepsilon_p) f(p_m, \varepsilon_p, p_{atm}, T_{atm}) n p_m\end{aligned} \tag{2}$$

where

$$\begin{aligned}&f(p_m, \varepsilon_p, p_{atm}, T_{atm})\\ &\quad = \frac{V_d}{120 p_{atm}\sqrt{RT_{atm}}} \frac{1}{\beta\left(\dfrac{p_m}{(1+\varepsilon_p)p_{atm}}\right)}.\end{aligned}$$

If we assume to know p_{atm} and T_{atm}, Eq. (2) gives all the possible values $(\varepsilon_p, \varepsilon_{\eta_v}, A^0_{th})$, which enable the model to return the given measured crank-shaft speed n, throttle plate angle α and measured manifold pressure p_m. Assuming to

[2] Hypothesis (H) is not restrictive since steady-state situations are usually encountered during engine operation, and reasonably simple tests are available on the on-board computer to detect steady-state operation. Moreover, as shown in (Hendricks and Sorenson (1990)), the manifold pressure in steady-states distributes uniformly around the mean values with quite small standard deviations. Note also that even if the engine model is intrinsically hybrid (Balluchi, Benvenuti, Di Benedetto, Pinello, & Sangiovanni-Vincentelli, 2000), hypothesis (H) allows us to neglect the hybrid nature of the SI engine since we will use this model in the case of constant crank-shaft speed and constant pressure.

reach three different steady-state situations, say $(n^1, \alpha^1, p_{\rm m}^1)$, $(n^2, \alpha^2, p_{\rm m}^2)$, $(n^3, \alpha^3, p_{\rm m}^3)$, then it is possible to find the values $(\varepsilon_{\rm p}, \varepsilon_{\eta_{\rm v}}, A_{\rm th}^0)$ that satisfy Eq. (2) for the three different cases. To do this, define

$$A_{\rm e,th}^i := A_{\rm e,th}(\alpha^i), \quad E_{\eta_{\rm v}} := (1 + \varepsilon_{\eta_{\rm v}})$$

and

$$h^i(\varepsilon_{\rm p}) := \eta_{\rm v}^{\rm est}(n^i, p_{\rm m}^i, \varepsilon_{\rm p}) f(p_{\rm m}^i, \varepsilon_{\rm p}, p_{\rm atm}, T_{\rm atm}) n^i p_{\rm m}^i$$

so that Eq. (2), for the three steady-state situations, gives

$$(A_{\rm e,th}^i + A_{\rm th}^0)(1 + \varepsilon_{\rm p}) = h^i(\varepsilon_{\rm p}) E_{\eta_{\rm v}}, \quad i = 1,2,3. \tag{3}$$

We can rewrite (3) as

$$\begin{cases} \displaystyle\sum_{i=1}^{3} (A_{\rm e,th}^{(i+1)\bmod 3} - A_{\rm e,th}^{(i+2)\bmod 3}) h^i(\varepsilon_{\rm p}) = 0, \\ E_{\eta_{\rm v}} = \dfrac{A_{\rm e,th}^i - A_{\rm e,th}^j}{h^i(\varepsilon_{\rm p}) - h^j(\varepsilon_{\rm p})}(1 + \varepsilon_{\rm p}), \quad i \neq j, \\ A_{\rm th}^0 = \dfrac{h^j(\varepsilon_{\rm p}) A_{\rm e,th}^i - h^i(\varepsilon_{\rm p}) A_{\rm e,th}^j}{h^i(\varepsilon_{\rm p}) - h^j(\varepsilon_{\rm p})}, \quad i \neq j \end{cases}$$

or

$$\begin{cases} \varphi(\varepsilon_{\rm p}) = 0, \\ E_{\eta_{\rm v}} = \phi_{ij}(\varepsilon_{\rm p}), \quad i \neq j, \\ A_{\rm th}^0 = \psi_{ij}(\varepsilon_{\rm p}), \quad i \neq j \end{cases}$$

with $i, j = 1,2,3$.

Then, an estimation $\hat{\varepsilon}_{\rm p}$ of the sensor error $\varepsilon_{\rm p}$ can be computed using an iterative process, for example Newton's method, to find the zeros of the function $\varphi(\varepsilon_{\rm p})$. Hence, we can compute the estimated values for $\hat{\varepsilon}_{\eta_{\rm v}}$, and the estimate $\hat{A}_{\rm th}^0$ as follows:

$$\hat{\varepsilon}_{\eta_{\rm v}} = \frac{1}{3} \sum_{\substack{i,j=1 \\ i>j}}^{3} \phi_{ij}(\hat{\varepsilon}_{\rm p}) - 1, \quad \hat{A}_{\rm th}^0 = \frac{1}{3} \sum_{\substack{i,j=1 \\ i>j}}^{3} \psi_{ij}(\hat{\varepsilon}_{\rm p}).$$

3.1.2. The case of unknown ambient pressure

In this case, we assume to measure the ambient pressure with the manifold sensor at key-on. Then we have $p_{\rm atm,m} = (1 + \varepsilon_{\rm p}) p_{\rm atm}$ and Eq. (2) reduces to

$$\begin{aligned} &A_{\rm e,th}(\alpha) + A_{\rm th}^0 \\ &\quad = (1 + \varepsilon_{\eta_{\rm v}}) \eta_{\rm v}^{\rm est}(n, p_{\rm m}, \varepsilon_{\rm p}) \tilde{f}(p_{\rm m}, p_{\rm atm,m}, T_{\rm atm}) n p_{\rm m}, \end{aligned} \tag{4}$$

where

$$\tilde{f}(p_{\rm m}, p_{\rm atm,m}, T_{\rm atm}) = \frac{V_{\rm d}}{120 p_{\rm atm,m} \sqrt{R T_{\rm atm}}} \frac{1}{\beta(p_{\rm m}/p_{\rm atm,m})}.$$

Assuming, as before, to reach three different steady-state situations, it is possible to find the values $(\varepsilon_{\rm p}, \varepsilon_{\eta_{\rm v}}, A_{\rm th}^0)$ that satisfy Eq. (4) for the three different cases. Consider, as before, the functions $A_{\rm e,th}^i$, $E_{\eta_{\rm v}}$ and define

$$\tilde{h}^i(\varepsilon_{\rm p}) := \eta_{\rm v}^{\rm est}(n^i, p_{\rm m}^i, \varepsilon_{\rm p}) \tilde{f}(p_{\rm m}^i, p_{\rm atm,m}, T_{\rm atm}) n^i p_{\rm m}^i$$

so that Eq. (4), for the three steady-state situations, gives

$$A_{\rm e,th}^i + A_{\rm th}^0 = \tilde{h}^i(\varepsilon_{\rm p}) E_{\eta_{\rm v}}, \quad i = 1,2,3. \tag{5}$$

We rewrite (5) as

$$\begin{cases} \displaystyle\sum_{i=1}^{3} (A_{\rm e,th}^{(i+1)\bmod 3} - A_{\rm e,th}^{(i+2)\bmod 3}) \tilde{h}^i(\varepsilon_{\rm p}) = 0, \\ E_{\eta_{\rm v}} = \dfrac{A_{\rm e,th}^i - A_{\rm e,th}^j}{\tilde{h}^i(\varepsilon_{\rm p}) - \tilde{h}^j(\varepsilon_{\rm p})}, \quad i \neq j, \\ A_{\rm th}^0 = \dfrac{\tilde{h}^j(\varepsilon_{\rm p}) A_{\rm e,th}^i - h^i(\varepsilon_{\rm p}) A_{\rm e,th}^j}{\tilde{h}^i(\varepsilon_{\rm p}) - \tilde{h}^j(\varepsilon_{\rm p})}, \quad i \neq j \end{cases}$$

or

$$\begin{cases} \tilde{\varphi}(\varepsilon_{\rm p}) = 0, \\ E_{\eta_{\rm v}} = \tilde{\phi}_{ij}(\varepsilon_{\rm p}), \quad i \neq j, \\ A_{\rm th}^0 = \tilde{\psi}_{ij}(\varepsilon_{\rm p}), \quad i \neq j \end{cases}$$

for $i, j = 1,2,3$.

Hence, as in the previous case, an estimation $\hat{\varepsilon}_{\rm p}$ of the sensor error $\varepsilon_{\rm p}$ can be easily computed. Finally, we have

$$\hat{\varepsilon}_{\eta_{\rm v}} = \frac{1}{3} \sum_{\substack{i,j=1 \\ i>j}}^{3} \tilde{\phi}_{ij}(\hat{\varepsilon}_{\rm p}) - 1, \quad \hat{A}_{\rm th}^0 = \frac{1}{3} \sum_{\substack{i,j=1 \\ i>j}}^{3} \tilde{\psi}_{ij}(\hat{\varepsilon}_{\rm p}).$$

It is worth noting that this method relies on the fact that $p_{\rm atm}$ does not varies significantly between key-on and the three different steady-state measurements. This may be not the case when driving in mountainous areas, so that in this case an estimation error would appear due to the variability of $p_{\rm atm}$.

3.2. Air-flow estimation

Once the estimations $\hat{\varepsilon}_{\rm p}$, $\hat{\varepsilon}_{\eta_{\rm v}}$ and $\hat{A}_{\rm th}^0$ are obtained, an estimation of the air-mass flow entering the cylinders can be computed using (A.5) and (A.2) as

$$\hat{\dot{m}}_{{\rm a},i} = \frac{\tilde{\dot{m}}_{\rm a}(\hat{\varepsilon}_{\rm p}, \hat{\varepsilon}_{\eta_{\rm v}}) + \tilde{\dot{m}}_{\rm a,th}(\hat{\varepsilon}_{\rm p}, \hat{A}_{\rm th}^0)}{2 n_{\rm c}}, \quad i = 1, \ldots, n_{\rm c}, \tag{6}$$

where

$$\tilde{\dot{m}}_{\rm a}(\hat{\varepsilon}_{\rm p}, \hat{\varepsilon}_{\eta_{\rm v}}) = \frac{V_{\rm d}}{120 R T_{\rm atm}} n \frac{p_{\rm m}}{(1 + \hat{\varepsilon}_{\rm p})} (1 + \hat{\varepsilon}_{\eta_{\rm v}}) \eta_{\rm v}^{\rm est}(n, p_{\rm m}, \hat{\varepsilon}_{\rm p})$$

and

$$\tilde{\dot{m}}_{\rm a,th}(\hat{\varepsilon}_{\rm p}, \hat{A}_{\rm th}^0) = \frac{p_{\rm atm}(A_{\rm e,th}(\alpha) + \hat{A}_{\rm th}^0)}{\sqrt{R\, T_{\rm atm}}} \beta\left(\frac{p_{\rm m}}{(1 + \hat{\varepsilon}_{\rm p})\, p_{\rm atm}}\right)$$

in the case of known ambient pressure, or

$$\tilde{\dot{m}}_{\mathrm{a,th}}(\hat{\varepsilon}_{\mathrm{p}}, \hat{A}^0_{\mathrm{th}}) = \frac{p_{\mathrm{atm,m}}\left(A_{\mathrm{e,th}}(\alpha) + \hat{A}^0_{\mathrm{th}}\right)}{(1+\hat{\varepsilon}_{\mathrm{p}})\sqrt{R\,T_{\mathrm{atm}}}}\beta\left(\frac{p_{\mathrm{m}}}{p_{\mathrm{atm,m}}}\right),$$

when the ambient pressure is measured. It is worth noting that, from the steady-state hypothesis (H), one should have $\tilde{\dot{m}}_{\mathrm{a}} = \tilde{\dot{m}}_{\mathrm{a,th}}$.[3]

4. The estimation of the fuel-to-air ratios γ_i

The problem solved in this section is the estimation of the F/A ratios $\gamma_i(t)$, $i = 1, \ldots, n_{\mathrm{c}}$, given by (1), from the output signal $\gamma(t)$, obtained from a single UEGO sensor. In the following subsection, we derive first a model of the exhaust gases during their motion from the cylinders to the oxygen sensor. Then, an estimation algorithm for $\dot{m}_{\mathrm{f},i}$ is proposed.

4.1. Mathematical model of the exhaust manifold

In this section, we develop a model for an n_{c}-cylinder engine describing the contribution in each cycle of each cylinder to the measured F/A ratio. We take into account the mixing among the air–fuel charges associated with each cylinder and the time that a single air–fuel charge takes to travel the length of its exhaust manifold runner. The UEGO sensor dynamics are also considered.

During engine operation, four events take place, i.e. intake, compression, combustion and exhaust. As previously explained, under hypothesis (H) the hybrid nature of the engine can be neglected. Moreover, since we are studying the exhaust gas dynamics, *the exhaust phase will be considered the starting event of the engine dynamics*. Referring to the ith cylinder, at the beginning of the exhaust process the exhaust valve opens, and the burnt gas goes from the high pressure environment in the cylinder to the lower pressure in the exhaust manifold. During this process, the exhaust gas expands into the exhaust manifold volume and travels towards the UEGO sensor. Note that in the exhaust stroke, most of the burnt gas in the cylinder is pushed out into the exhaust manifold by the piston.

When the gas moves in the exhaust manifold the main processes that must be taken into account are

(1) the transport of the burnt gases in the exhaust manifold runner;
(2) the gas-mixing in the manifold junctions.

The transport delays associated with each of the n_{c} exhaust runners are not equal, since each runner has a different length. Moreover, during the gas transport, the gas molecule velocities spread about the mean value. While it is not difficult, although mathematically involved, to consider these aspects, for the sake of simplicity, we will assume that the delays are all equal to a quantity δ_{r}, and we will neglect the velocity dispersion. The effect of the delay differences will be analyzed by a set of simulations. The mixing process can be seen as a merging process at the runner confluence, where the mixture flows sum up. Hence, the merging process during the travelling towards the sensor will be modelled by a first-order system. In summary, the main processes which take place in the exhaust manifold can be taken into account by the following transfer function:

$$P_{\mathrm{MIX}}(s) = \frac{\mathrm{e}^{-\delta_{\mathrm{r}} s}}{1+\tau_{\mathrm{MIX}} s} \tag{7}$$

with δ_{r}, τ_{MIX} the transport delay and the time constants of the mixing process. Under the assumption of plug flow in the exhaust manifold, the average velocity of the exhaust gases is proportional to the engine speed (Chang et al., 1995; Jones et al., 1995). Thus, the transport delay δ_{r} can be assumed inversely proportional to the crank-shaft speed (Choi & Hedrick, 1998; Grizzle et al., 1991; Powell et al., 1981)

$$\delta_{\mathrm{r}} = \frac{k}{n}.$$

However, when the sensor is located close to the exhaust valve, the blast of exhaust gases during the blow down process dominates the transport delay. As a consequence, the exhaust transport delay can be assumed constant (as shown in Table 1 in Jones et al., 1995).

The UEGO sensor has desirable properties, since it is linear, accurate and gives fast responses. As far as its modelling is concerned, the diffusion process of the oxygen that occurs in the UEGO sensor can be modelled as a first-order system with a diffusion delay (Chang et al., 1995; Fekete, Nester, Gruden, & Powell, 1995). Hence, the UEGO sensor dynamics are represented by the following transfer function:

$$P_{\mathrm{UEGO}}(s) = \frac{\mathrm{e}^{-\delta_{\mathrm{UEGO}} s}}{1+\tau_{\mathrm{UEGO}} s} \tag{8}$$

with δ_{UEGO}, τ_{UEGO} the diffusion delay and time constant of the diffusion process. As shown in Jones et al. (1995), the sensor's time constant τ_{UEGO} varies with the throttle angle but not with the engine speed.

The F/A ratio at the runner confluence is a *known* function

$$\gamma_{\mathrm{c}}(t) = f(\gamma_1(t), \ldots, \gamma_{n_{\mathrm{c}}}(t))$$

of the ratios $\gamma_i(t)$. In fact, since the air-mass flow $\dot{m}_{\mathrm{a},i}$ entering each cylinder is the same, $\gamma_{\mathrm{c}}(t)$ depends only on the ratios $\gamma_i(t)$, on the number n_{c} of cylinders and on the timing of the exhaust process of each cylinder. When the only charge present at the UEGO sensor at time t is the ith one, f is simply given by the value $\gamma_i(t)$, while it is given by the arithmetic mean between $\gamma_i(t)$, $\gamma_j(t)$ when the charges present at the UEGO sensor at time t are the ith and jth ones. More precisely, let T be the time required for the

[3] In fact, $(\hat{\varepsilon}_{\mathrm{p}}, \hat{\varepsilon}_{\eta_{\mathrm{v}}}, \hat{A}^0_{\mathrm{th}})$ are defined as the solutions of the equations $\tilde{\dot{m}}_{\mathrm{a}}(\hat{\varepsilon}_{\mathrm{p}}, \hat{\varepsilon}_{\eta_{\mathrm{v}}}) = \tilde{\dot{m}}_{\mathrm{a,th}}(\hat{\varepsilon}_{\mathrm{p}}, \hat{A}^0_{\mathrm{th}})$. In (6) we considered the mean between the values of $\tilde{\dot{m}}_{\mathrm{a}}$ and $\tilde{\dot{m}}_{\mathrm{a,th}}$ in order to reduce influences of possible estimation errors on $\hat{\varepsilon}_{\mathrm{p}}$, $\hat{\varepsilon}_{\eta_{\mathrm{v}}}$, $\hat{A}^0_{\mathrm{th}}$. A study on parameter sensibility may help in fixing a more appropriated weighted average to compute $\hat{\dot{m}}_{\mathrm{a},i}$.

Table 1
Maximum number of independent samplings obtainable for critical speeds n

Critical speed n (rpm)	Independent samplings
1579	19
1667	18
1765	17
1875	16
2000	15
2143	14
2308	13
2500	12
2727	11
3000	10
3158	19
3333	9
3529	17
3750	8
4000	15
4286	7
4615	13
4737	19
5000	6
5294	17
5455	11
5625	16
6000	5

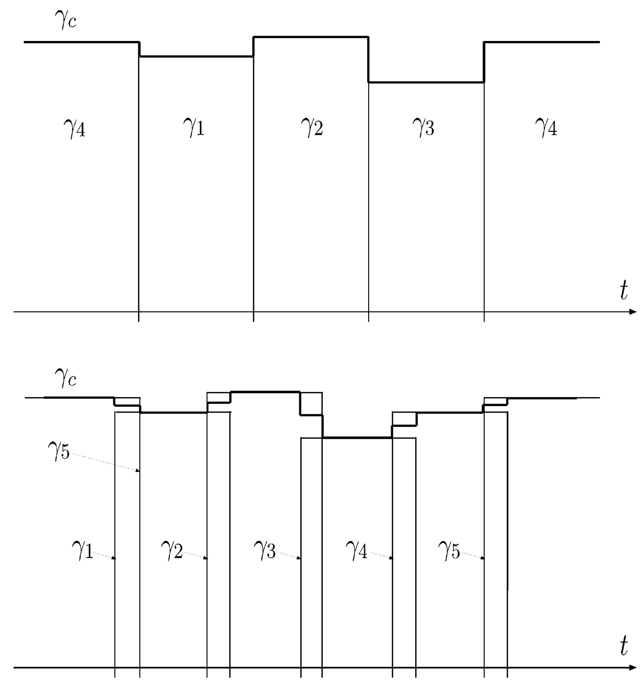

Fig. 1. Normalized F/A ratio $\gamma_c(t)$ at the runner confluence (four- and five-cylinders engines).

crank-shaft to advance 720°. Then, each phase takes $T/4$ time and the cycles of two subsequent cylinders are shifted by T/n_c. Therefore, when $n_c > 4$ the contributions to $\gamma_c(t)$ due to two subsequent cylinders i, $i+1$ overlap for a time

$$\Delta = \frac{T}{\text{l.c.m. } (4, n_c)}$$

and, during this overlap, we have

$$\gamma_c(t) = \frac{\gamma_i(t) + \gamma_{i+1}(t)}{2}.$$

The function $\gamma_c(t)$ is clearly a piece-wise periodic function of period Δ. In the case of four and five cylinders one has the pictures shown in Fig. 1.

On the basis of the previous discussion, the measured normalized F/A mixture ratio $\gamma(t)$ can be obtained from

$$\gamma(s) = P(s)\gamma_c(s) \tag{9}$$

where

$$P(s) = \frac{e^{-\delta s}}{(1+\tau_{\text{MIX}}s)(1+\tau_{\text{UEGO}}s)}, \qquad \delta = \frac{k}{n} + \delta_{\text{UEGO}}$$

is the transfer function describing the dynamics of the exhaust manifold, obtained using (7) and (8).

4.2. *The estimation algorithm: the ideal case*

The dependence of the piece-wise constant signal $\gamma_c(t)$ on the time interval Δ suggests to look for a solution of the problem in the discrete-time context, by considering a sample rate equal to Δ and a discrete-time signal $\gamma_c(q)$ followed by a zero-order holder. The discrete-time signal $\gamma_c(q)$ is shown in Fig. 2 in the case of four and five cylinders.

From (9) and considering the inverse Laplace transform, we obtain

$$\gamma(t+\delta) = \mathscr{L}^{-1}\left[\frac{1}{(1+\tau_{\text{MIX}}s)(1+\tau_{\text{UEGO}}s)}\gamma_c(s)\right].$$

Since γ_c can be seen as a discrete-time signal followed by a zero-order holder, we consider the sampling $\gamma_s(q)$ of the signal $\gamma(t+\delta)$, with period Δ. Hence, we have

$$\gamma_s(q) = \mathscr{Z}^{-1}[Q(z)\gamma_c(z)],$$

where $Q(z)$ is the transfer function of the sampled system, consisting of the zero-order holder, the mixing and sensor dynamics, and the sampler

$$\begin{aligned} Q(z) &= \mathscr{Z}\left[\mathscr{L}^{-1}\left[\frac{1}{(1+\tau_{\text{MIX}}s)(1+\tau_{\text{UEGO}}s)}\frac{1}{s}\right]\Bigg|_{t=k\Delta}\right] \\ &\quad \times \frac{z-1}{z} \\ &= 1 - \frac{\tau_{\text{MIX}}}{\tau_{\text{MIX}}-\tau_{\text{UEGO}}}\frac{z-1}{z-p_1} \\ &\quad + \frac{\tau_{\text{UEGO}}}{\tau_{\text{MIX}}-\tau_{\text{UEGO}}}\frac{z-1}{z-p_2} \end{aligned} \tag{10}$$

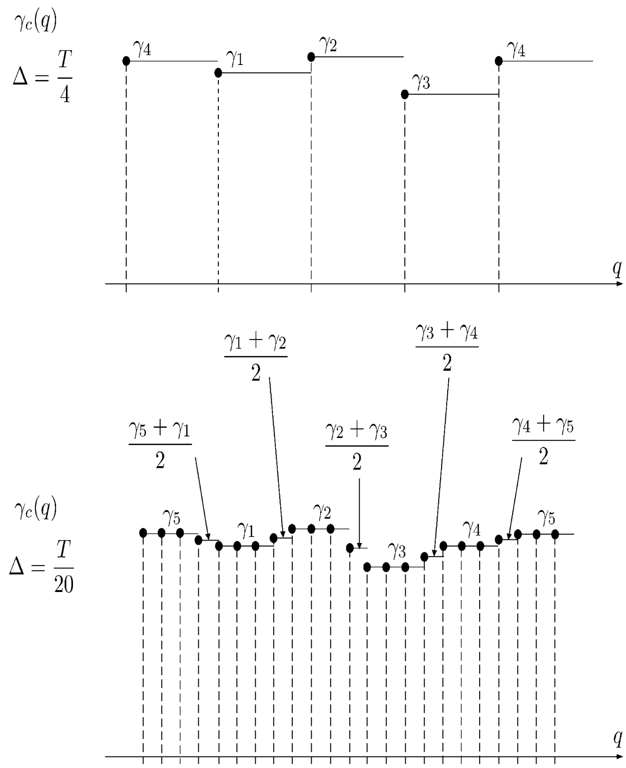

Fig. 2. $\gamma_c(q)$ in the case of four and five cylinders.

with

$$p_1 = e^{-\Delta/\tau_{MIX}}, \quad p_2 = e^{-\Delta/\tau_{UEGO}}.$$

Note that we consider $\gamma(t+\delta)$ and not $\gamma(t)$ since the total delay δ, depending on the crank-shaft speed and the UEGO sensor characteristics, is a known quantity. Therefore, it is possible to compensate for the presence of this delay in the estimation algorithm and to work directly on the signal $\gamma(t+\delta)$.

In what follows, in order to illustrate the procedure, we consider two interesting cases, the four- and five-cylinders engines.

4.2.1. A simple case: a four-cylinders engine

In the case of a four-cylinders engine $\Delta = T/4$ and the contributions $\gamma_i(t)$ do not overlap, see Fig. 1. Referring to Fig. 2, the $\mathscr{Z}$-transformation of the signal $\gamma_c(q)$ is given by

$$\gamma_c(z) = \mathscr{Z}[\gamma_c(q)] = \gamma_1 \frac{z^4}{z^4-1} + \gamma_2 \frac{z^3}{z^4-1} + \gamma_3 \frac{z^2}{z^4-1} + \gamma_4 \frac{z}{z^4-1}. \tag{11}$$

Considering the transfer function (10) and input (11) it is possible to compute the output

$$\gamma_s(z) = \mathscr{Z}[\gamma_s(q)] = Q(z)\gamma_c(z). \tag{12}$$

This output has the form

$$\gamma_s(z) = \gamma_{st}(z) + \gamma_{ss}(z) = \frac{R_1 z^2 + R_2 z + R_3}{(z-p_1)(z-p_2)} + \frac{z}{z^4-1}\sum_{j=1}^{4} \gamma_{ss,j}\, z^{4-j}, \tag{13}$$

where $\gamma_{ss}(z)$, $\gamma_{st}(z)$ are the $\mathscr{Z}$-transformations of the steady-state and transient components $\gamma_{st}(q)$, $\gamma_{ss}(q)$ of the output $\gamma_s(q)$, and R_1, R_2, R_3 are appropriate constants. Comparing (12) and (13) one gets

$$A_4 \begin{pmatrix} \gamma_1 \\ \gamma_2 \\ \gamma_3 \\ \gamma_4 \end{pmatrix} = B_4 \begin{pmatrix} \gamma_{ss,1} \\ \gamma_{ss,2} \\ \gamma_{ss,3} \\ \gamma_{ss,4} \end{pmatrix}, \tag{14}$$

where

$$A_4 = \begin{pmatrix} a_1 & a_2 & 0 & 0 \\ 0 & a_1 & a_2 & 0 \\ 0 & 0 & a_1 & a_2 \\ a_2 & 0 & 0 & a_1 \end{pmatrix}, \quad B_4 = \begin{pmatrix} b_1 & b_2 & 1 & 0 \\ 0 & b_1 & b_2 & 1 \\ 1 & 0 & b_1 & b_2 \\ b_2 & 1 & 0 & b_1 \end{pmatrix}$$

with

$$a_1 = \frac{\tau_{UEGO}}{\tau_{MIX}-\tau_{UEGO}}(1-p_2)p_1 - \frac{\tau_{MIX}}{\tau_{MIX}-\tau_{UEGO}}(1-p_1)p_2,$$

$$a_2 = -\frac{\tau_{UEGO}}{\tau_{MIX}-\tau_{UEGO}}(1-p_2) + \frac{\tau_{MIX}}{\tau_{MIX}-\tau_{UEGO}}(1-p_1),$$

$$b_1 = p_1 p_2, \quad b_2 = -(p_1+p_2).$$

Eq. (14) represents the relationship existing between the measured signal $\gamma_{ss,j}$, $j = 1,\dots,4$, at the steady-state and the F/A ratios γ_j released by each cylinder during the exhaust phase. This equation can be solved for the γ_j's; for, we note that A_4^{-1} exists when

$$(1+2a+p_1)p_2 + (1+2b)p_1 + b + a \neq 0,$$

$$a = -\frac{\tau_{MIX}}{\tau_{MIX}-\tau_{UEGO}}, \quad b = \frac{\tau_{UEGO}}{\tau_{MIX}-\tau_{UEGO}}$$

namely almost always.

The structure of the matrices in (14) reflects the physics of the exhaust dynamics. The input contributions to $\gamma_{ss,j}$ is distributed among the four cylinders, and the a_i's, b_i's determine the corresponding percentage of contribution. In fact, the runners are supposed to have the same geometry, so that the contribution of the ith cylinder to $\gamma_{ss,j}$ is equal to the contribution of the $(i+1)$th cylinder to $\gamma_{ss,j+1}$.

4.2.2. The five-cylinders case

In the case of a five-cylinders engine $\Delta = T/20$ and the contributions $\gamma_i(t)$ do overlap, as shown in Fig. 1. Considering Fig. 2, we have

$$\begin{aligned}\gamma_c(z) = {} & \frac{\gamma_1+\gamma_5}{2}\frac{z^{20}}{z^{20}-1} + \gamma_1\frac{z^{19}}{z^{20}-1} + \gamma_1\frac{z^{18}}{z^{20}-1} \\ & + \gamma_1\frac{z^{17}}{z^{20}-1} + \frac{\gamma_2+\gamma_1}{2}\frac{z^{16}}{z^{20}-1} + \gamma_2\frac{z^{15}}{z^{20}-1} \\ & + \gamma_2\frac{z^{14}}{z^{20}-1} + \gamma_2\frac{z^{13}}{z^{20}-1} + \frac{\gamma_3+\gamma_2}{2}\frac{z^{12}}{z^{20}-1} \\ & + \gamma_3\frac{z^{11}}{z^{20}-1} + \gamma_3\frac{z^{10}}{z^{20}-1} + \gamma_3\frac{z^{9}}{z^{20}-1} \\ & + \frac{\gamma_4+\gamma_3}{2}\frac{z^{8}}{z^{20}-1} + \gamma_4\frac{z^{7}}{z^{20}-1} + \gamma_4\frac{z^{6}}{z^{20}-1} \\ & + \gamma_4\frac{z^{5}}{z^{20}-1} + \frac{\gamma_4+\gamma_5}{2}\frac{z^{4}}{z^{20}-1} + \gamma_5\frac{z^{3}}{z^{20}-1} \\ & + \gamma_5\frac{z^{2}}{z^{20}-1} + \gamma_5\frac{z}{z^{20}-1},\end{aligned}$$

which has to be put in (12). Reasoning as in the four cylinders case, we can write

$$\begin{aligned}\gamma_s(z) = \gamma_{st}(z) + \gamma_{ss}(z) = {} & \frac{R_1z^2+R_2z+R_3}{(z-p_1)(z-p_2)} \\ & + \frac{z}{z^{20}-1}\sum_{j=1}^{20}\gamma_{ss,j}z^{20-j}.\end{aligned}$$

Comparing the two expressions for $\gamma_s(z)$ and using the same notation of the previous subsection, we finally determine

$$A_5\begin{pmatrix}\gamma_1\\ \vdots\\ \gamma_5\end{pmatrix} = B_5\begin{pmatrix}\gamma_{ss,1}\\ \vdots\\ \gamma_{ss},20\end{pmatrix}, \qquad (15)$$

where

$$A_5 = \begin{pmatrix} c_4 & 0 & 0 & 0 & c_5\\ c_1 & 0 & 0 & 0 & 0\\ c_1 & 0 & 0 & 0 & 0\\ c_2 & c_3 & 0 & 0 & 0\\ c_5 & c_4 & 0 & 0 & 0\\ 0 & c_1 & 0 & 0 & 0\\ 0 & c_1 & 0 & 0 & 0\\ 0 & c_2 & c_3 & 0 & 0\\ 0 & c_5 & c_4 & 0 & 0\\ 0 & 0 & c_1 & 0 & 0\\ 0 & 0 & c_1 & 0 & 0\\ 0 & 0 & c_2 & c_3 & 0\\ 0 & 0 & c_5 & c_4 & 0\\ 0 & 0 & 0 & c_1 & 0\\ 0 & 0 & 0 & c_1 & 0\\ 0 & 0 & 0 & c_2 & c_3\\ 0 & 0 & 0 & c_5 & c_4\\ 0 & 0 & 0 & 0 & c_1\\ 0 & 0 & 0 & 0 & c_1\\ c_3 & 0 & 0 & 0 & c_2 \end{pmatrix},$$

$$B_5 = \begin{pmatrix} b_1 & b_2 & 1 & 0 & \cdots & 0 & 0\\ 0 & b_1 & b_2 & 1 & \cdots & 0 & 0\\ \vdots & \vdots & \ddots & \ddots & \ddots & & \vdots\\ 0 & & & \cdots & b_1 & b_2 & 1\\ 1 & 0 & & \cdots & 0 & b_1 & b_2\\ b_2 & 1 & 0 & \cdots & 0 & 0 & b_1 \end{pmatrix}$$

with

$$c_1 = (1-p_1)(1-p_2),$$

$$c_2 = -(p_1-1)(p_2-\tfrac{1}{2})a - (p_1-\tfrac{1}{2})(p_2-1)b,$$

$$c_3 = \tfrac{1}{2}(p_1-1)a + \tfrac{1}{2}(p_2-1)b,$$

$$c_4 = -(p_1-1)(\tfrac{1}{2}p_2-1)a - (\tfrac{1}{2}p_1-1)(p_2-1)b,$$

$$c_5 = -\tfrac{1}{2}(p_1-1)p_2a - \tfrac{1}{2}p_1(p_2-1)b.$$

As in the four-cylinders case, the regular structure in this relation reflects the physics of the exhaust dynamics, with the input contributions to $\gamma_{ss,j}$ distributed among the five cylinders.

Note that (15) can be solved with respect to the estimates γ_i because the matrix A_5 has a left pseudo inverse almost always.

4.3. The estimation algorithm: practical implementation

In order to implement the estimation algorithm, we have to consider the constraints due to the sampling period of the central control unit (CCU). Let us assume that the UEGO sensor measurements are sampled with a sampling period Δ_s. In general $\Delta_s \neq \Delta$, so that the desired output measurements $\gamma_{ss,i}$ can be obtained by interpolating the sampled output measurements; note that the number of the necessary measurements is given by

$$n_s = \text{l.c.m.}\ (4, n_c)$$

so that the CCU has to sample the output for a period $n_s\Delta_s$. Obviously, this period can be greater than the period T in which a cycle takes place. Since the steady-state output is a periodic signal over T, we can get the desired measurements from subsequent cycles. Since we have to ensure independent measurements, when $n_s\Delta_s > T$ the following must hold

$$h\Delta_s \neq kT, \quad h = 1,\ldots,n_s, \ \ k = 1,\ldots,\bar{k},$$

where $\bar{k}$ is smallest integer such that $n_s\Delta_s < \bar{k}T$. In fact, this condition ensures that two samplings do not occur at the same instant $t \bmod T$. Since n_s, Δ_s are given, there exist particular values for the crank-shaft speed that do not allow to have independent measurements. For example, in a five-cylinders engine, for which $n_s = 20$, and for $\Delta_s = 4$ ms when $n \leqslant 1500$ rpm the samplings are independent; for higher speeds these samplings are not all independent, and in Table 1 are reported the maximum number of independent samplings obtainable for the critical speeds.

Note also that the hypothesis of steady-state measurements is not restrictive since steady-state situations are usually encountered in the engine behavior, and reasonably simple tests are available on the on-board CCU to detect steady-state situations. Moreover, in order to minimize the estimation error, when the steady-state conditions are maintained for a sufficiently long period of time we can use mn_s samplings and compute the mean value for each sampling over m different measurements.

Finally, in the ideal case, Eqs. (14) and (15) can be solved with respect to γ_i in an analytic way. In the real case, in order to minimize the error due to parameter uncertainties and noise, a least square algorithm is used. Therefore, one obtains

$$\begin{pmatrix} \hat{\gamma}_1 \\ \hat{\gamma}_2 \\ \hat{\gamma}_3 \\ \hat{\gamma}_4 \end{pmatrix} = (A_4^T A_4)^{-1} A_4^T B_4 \begin{pmatrix} \gamma_{ss,1} \\ \gamma_{ss,2} \\ \gamma_{ss,3} \\ \gamma_{ss,4} \end{pmatrix} \tag{16}$$

in the case of four-cylinders, and

$$\begin{pmatrix} \hat{\gamma}_1 \\ \hat{\gamma}_2 \\ \hat{\gamma}_3 \\ \hat{\gamma}_4 \\ \hat{\gamma}_5 \end{pmatrix} = (A_5^T A_5)^{-1} A_5^T B_5 \begin{pmatrix} \gamma_{ss,1} \\ \vdots \\ \gamma_{ss,20} \end{pmatrix} \tag{17}$$

in the case of five-cylinders.

5. Injector characteristics estimation

In this section, we obtain an estimate of the injector characteristics g_i, $T_{i,\text{off}}$. Once the air-flow mass $\hat{\dot{m}}_{a,i}$ and the F/A ratios $\hat{\gamma}_i$, $i = 1,\ldots,n_c$, have been estimated with (6) and (16) or (7), from (1) we obtain the estimates of the injected fuel mass

$$\hat{\dot{m}}_{f,i} = \hat{\gamma}_i(t)\hat{\dot{m}}_{a,i}, \quad i = 1,\ldots,n_c. \tag{18}$$

From this relation it is possible to determine the injector characteristics g_i and $T_{i,\text{off}}$, solution of Eq. (A.7) with $\dot{m}_{f,i}$ replaced by (18) for each steady-state situation. One can easily estimate the injector characteristics

$$\hat{g}_i = 10 \sum_{k=1}^{3} \frac{n^k \hat{\dot{m}}_{f,i}^j - n^j \hat{\dot{m}}_{f,i}^k}{n^k n^j (T_i^j - T_i^k)}, \quad i = 1,\ldots,n_c,$$

$$\hat{T}_{i,\text{off}} = \frac{1}{3} \sum_{k=1}^{3} \frac{T_i^k n^k \hat{\dot{m}}_{f,i}^j - T_i^j n^j \hat{\dot{m}}_{f,i}^k}{n^k \hat{\dot{m}}_{f,i}^j - n^j \hat{\dot{m}}_{f,i}^k},$$

where $j = (k+1) \bmod 3$ and the superscript $k = 1, 2, 3$ corresponds to a steady-state situation.

6. Experimental results

Ideally, the quality of the approach should be assessed on a real engine. However, confidentiality about engine parameters and injector characteristics requested by our industrial partners together with the difficulty of setting up the appropriate instrumentation, made validation on a real engine unfeasible. For this reason, we limit our discussion of experimentation on simulation results. We made sure that the simulation parameters and the results obtained were consistent with reality by having the approach scrutinized by Magneti Marelli experts who directed the selection of the critical parts of the experiments. It is conforting that this estimation approach will be adopted in future industrial engine management systems.

The estimation algorithms for the F/A ratios and for the injector characteristics were applied separately to the data obtained from a simulation, to test their efficiency with respect to the precision of the available measurements.

As far as the F/A ratios are concerned, the estimation algorithm has been applied to the data supplied by a model of the exhaust manifold for a five-cylinders engine with runners of different length. This was modelled by choosing a different gain k for each runner delay $\delta_r = k/n$. The engine speed is equal to 5000 rpm. It is assumed that there is a complete air–fuel maldistributions, that is

$$(\gamma_1 \;\; \gamma_2 \;\; \gamma_3 \;\; \gamma_4 \;\; \gamma_5) = (0.90 \;\; 0.93 \;\; 1.10 \;\; 1.08 \;\; 1.00).$$

and the model parameters are the following:

$$\delta_{r,1} = 5 \text{ ms}, \quad \delta_{r,2} = 5.125 \text{ ms}, \quad \delta_{r,3} = 5.25 \text{ ms},$$

$$\delta_{r,4} = 5.375 \text{ ms}, \quad \delta_{r,5} = 5.5 \text{ ms},$$

$$\tau_{MIX} = 10 \text{ ms}, \quad \tau_{UEGO} = 100 \text{ ms}, \quad \delta_{UEGO} = 10 \text{ ms}.$$

The mean value of the runners delays has been used in the estimation algorithm, that is $\bar{\delta}_r = 5.25$, so that $\delta = \delta_{UEGO} + \bar{\delta}_r = 15.3$ ms and the coefficient of matrices A_5 and B_5 in (15) result to be $b_1 = 0.8763$, $b_2 = -1.875$ and

$$c_1 = 13.488 \times 10^{-4}, \quad c_2 = 10.042 \times 10^{-4},$$

$$c_3 = 3.446 \times 10^{-4}, \quad c_4 = 10.191 \times 10^{-4},$$

$$c_5 = 3.2979 \times 10^{-4}.$$

In order to render the simulations more realistic we supposed that the signal measured by the UEGO sensor is affected by a noise, mainly due to the chaotic diffusion process. Moreover, we also considered a noise on the measured signal. The amplitudes of the white noises have been appropriately set so to obtain a simulated A/F UEGO output comparable with a signal measured on a real engine in the same operational situation. Fig. 3 shows the typical signal used in the simulation.

As explained in Section 4.3, better results can be obtained by considering mean values for each sampling over different

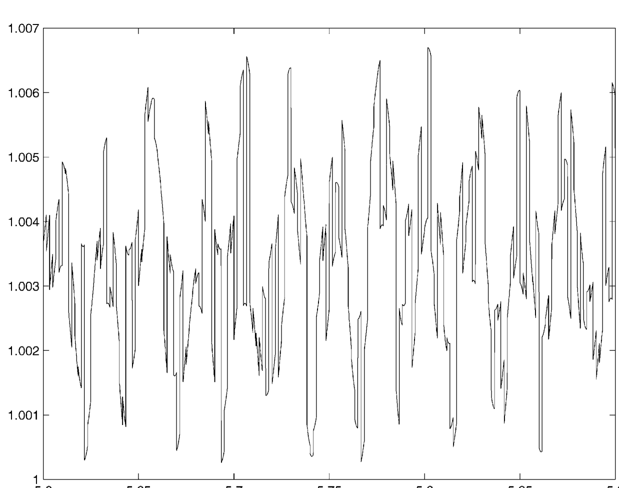

Fig. 3. UEGO sensor output used in simulation.

Table 2
Estimates $\hat{\gamma}_i$, $i = 1, \ldots, 5$

	Real value	Estimated value	Error %
γ_1	0.90	0.9007	0.08
γ_2	0.93	0.9327	0.29
γ_3	1.10	1.1007	0.07
γ_4	1.08	1.0707	0.86
γ_5	1.00	1.0109	1.09

Table 3
Simulation data

α (deg)	$A_{e,th}$ (mm^2)	n (rpm)	p_m (mbar)	T_i (ms)	A/F
67.50	431	2563	985	11.58	14.64
26.64	85	1464	904	9.90	14.66
20.70	48	2068	601	6.86	14.65

measurements, so minimizing the noise effects on UEGO measurements. Clearly, a tradeoff has to be done between the quality (and cost) of the UEGO sensor and the computational effort requested by the algorithm, which affects the cost of the central unit.

The result of the F/A ratios estimation algorithm (17) is summarized in Table 2.

As far as the injector characteristics are concerned, the estimation algorithm has been tested on the single ith injector for which it is known as A/F ratio. The data are obtained from a simulation and the values of the parameters of the model are

$$V_d = 1242 \text{ cm}^3, \quad p_{atm} = 1013 \text{ mbar}, \quad T_{atm} = 300 \text{ K},$$

$$R = 287 \text{ KJ/kg K}, \quad \mu_c = c_p/c_v = 1.4,$$

$$g_i = 1.93 \times 10^{-3} \text{ kg/s}, \quad T_{i,off} = 0.75 \text{ ms},$$

$$\eta_v^{est} = 0.597071 + 5.15605 \times 10^{-5} n + 9.30417 \times 10^{-7} p_{man}.$$

Moreover, we considered to have

$$\varepsilon_p = -1.237\%, \quad \varepsilon_{\eta_v} = 3.48\%, \quad A_{th}^0 = 2.95 \text{ mm}^2.$$

We consider the three steady-state conditions reported in Table 3, and the application of the estimation algorithm presented in Section 3 (for ε_p, ε_{η_v}, A_{th}^0 and for $\dot{m}_{a,i}$) and in Section 5 (for g_i and $T_{i,off}$) gives the results summarized in Table 4.

The estimation errors are due to the finite number of data digits used for the measurements. Consequently, these errors cannot be avoided unless the accuracy of the sensor is dramatically increased.

Finally, to take into account the effects of cascaded estimations on the overall estimation process, we considered

Table 4
Estimates

	Real value	Estimated value	Error %
g_i (g/s)	1.93	1.93	0.1
$T_{i,\text{off}}$ (ms)	0.75	0.75	0.6
ε_p (%)	−1.237	−1.239	0.1
$\varepsilon_{\eta_\text{v}}$ (%)	3.48	3.36	3.5
A^0_th (mm^2)	2.95	2.88	2.2

for the same case of Table 3 the higher estimation error obtained in the γ_i's estimation, namely an error of 1.10%. The values of the A/F in this new estimation are those in Table 3 multiplied by 1.011. In this case we obtained an error of 1.10% on g_i and 0.6% on $T_{i,\text{off}}$.

7. Conclusions

We presented an estimation technique for injector characteristics based on a set of measurements that can be carried out by the sensors present in the car, i.e. intake manifold pressure, crank-shaft speed, throttle-valve plate angle, injections timing and exhaust A/F ratio, which is measured by a single UEGO sensor placed at the exhaust pipe output.

The estimation strategy is based on a sequence of estimations of various quantities needed to estimate the characteristics of each injector. In particular, we have determined an estimation chain which yields good results when applied to simulated systems. We are in the process of transferring this approach to our industrial sponsors who are interested in adopting the estimation algorithm on industrial strength applications.

Acknowledgements

This research has been partially sponsored by Magneti Marelli, PARADES, a Cadence, Magneti Marelli and ST Microelectronics GEIE, and by the IST 2002 Columbus Project of the European Community. The authors are grateful to G. Gaviani, C. Rossi, R. Flora, G. Serra, C. Poggio and their teams at Magneti Marelli for having introduced the problem and for the many discussions. The authors also thank V. Nicoletti for his comments on the practical implementation of the estimation algorithm. We thank the anonymous reviewers who contributed many useful comments to improve the quality of the paper.

Appendix A. Mathematical model of the intake manifold for a spark ignition engine

In this appendix, we present the mathematical model of the intake manifold of a SI engine. We make use of the so-called Mean Value Model of a spark ignition engine (Aquino, 1981; Chaumerliac, Bidan, & Boverie, 1994; Dobner, 1980; Hendricks & Sorenson, 1990; Hendricks & Vesterholm, 1992), which describes the air dynamics with good accuracy without considering cycle variations. For the sake of simplicity, the temperature and transient heating effects are not explicitly taken into account.

The intake manifold dynamics describes the mean values of the relevant engine variables, i.e. the intake manifold pressure, the fuel flow-rate inside the cylinder and the crank-shaft speed with respect to variations of the engine inputs, namely the throttle plate angle and the injection pulse duration (the spark advance angle is assumed to be constant).

Throttle air mass flow rate equations: The average air-mass flow rate through the throttle $\dot m_{\text{a,th}}$ (kg/s) can be calculated (see Taylor & Taylor, 1970) as the air-mass flow $\dot m$ of a compressible fluid through a channel between two areas at different pressures:

$$\dot m = C_\text{d}\,\frac{p_1}{\sqrt{R\,T_1}}\,\frac{A_2}{\sqrt{1-A_2/A_1}}\,\beta\left(\frac{p_2}{p_1}\right), \tag{A.1}$$

where C_d is a discharge coefficient, R is the ideal gas constant for air (J K^{-1} kg^{-1}), A_i, p_i, T_i are the area, the pressure, the temperature of section i and

$$\beta\left(\frac{p_2}{p_1}\right)=\begin{cases}\sqrt{\dfrac{2\mu_\text{c}}{\mu_\text{c}-1}\left[\left(\dfrac{p_2}{p_1}\right)^{2/\mu_\text{c}}-\left(\dfrac{p_2}{p_1}\right)^{(\mu_\text{c}+1)/\mu_\text{c}}\right]} \\ \quad\text{if } \dfrac{p_2}{p_1}\geqslant r_{cr}, \\ \sqrt{\mu_\text{c}}\left(\dfrac{2}{\mu_\text{c}+1}\right)^{\frac{\mu_\text{c}+1}{2(\mu_\text{c}-1)}} \\ \quad\text{if } \dfrac{p_2}{p_1}< r_{cr}\end{cases}$$

with $r_{cr}=(2/\mu_\text{c}+1)^{\mu_\text{c}/(\mu_\text{c}-1)}$ and μ_c the specific heat ratio (J kg^{-1} K^{-1}).

If we assume the downstream section A_2 to be the throttle section and the upstream section A_1 a section just before the throttle, then $A_1 \gg A_2$ and Eq. (A.1) reduces to

$$\dot m_{\text{a,th}} = C_\text{d}\,\frac{p_\text{atm}}{\sqrt{R\,T_\text{atm}}}A_\text{th}(\alpha)\beta\left(\frac{p_\text{man}}{p_\text{atm}}\right), \tag{A.2}$$

where p_atm and T_atm are the ambient pressure (N m^{-2}) and the air temperature (K), p_man is the mean value intake manifold pressure (N m^{-2}), A_th is the throttle area (m^2), α the throttle plate angle (rad) and C_d the throttle discharge coefficient.

The mean value manifold pressure p_man can be determined from the average of a set of measurements, giving

$$p_\text{m} = (1+\varepsilon_\text{p})\,p_\text{man} \tag{A.3}$$

of the pressure, where $|\varepsilon_\text{p}| \leqslant 3\%$ is the estimate sensor error.

In the sequel we assume

$$C_d A_{th}(\alpha) = A_{e,th}(\alpha) + A_{th}^0, \tag{A.4}$$

where $A_{e,th}(\alpha)$ is the so-called equivalent throttle area and A_{th}^0 is the offset area, i.e. the area of the throttle when $\alpha = 0$, $A_{e,th}(0)=0$. It is assumed that $A_{th}^0 \in [0, 5]\ \mathrm{mm}^2$ is an unknown value slowly varying because of aging.

Engine air pumping equations: Theoretically, the average air-mass flow $\dot{m}_a$ (kg/s) entering the n_c cylinders of the engine is given by

$$\dot{m}_a = \rho_{air} \frac{V_d}{2} \frac{n}{60},$$

where ρ_{air} is the air density, V_d the displacement volume (m^3) and n the crank-shaft speed (rpm). By using the ideal gas equation for the air in the manifold

$$\frac{p_{man}}{\rho_{air}} = R\,T_{air} = R\,T_{atm}$$

and taking into account the real supply to the cylinders, we obtain $\dot{m}_a$ as a function of the crank-shaft speed n and of the mean value intake manifold pressure p_{man}

$$\dot{m}_a = \frac{V_d}{120 R T_{atm}}\, n\, p_{man} \eta_v(n, p_{man}), \tag{A.5}$$

where η_v is the so-called volumetric efficiency and it is assumed to be a function of n and p_{man}. In the sequel we will assume to know the volumetric efficiency up to a constant error $|\varepsilon_{\eta_v}| \leqslant 10\%$, i.e.

$$\eta_v(n, p_{man}) = (1 + \varepsilon_{\eta_v})\eta_v^{est}, (n, p_{man}), \tag{A.6}$$

where η_v^{est} is the estimated volumetric efficiency.

Fuel flow equations: The fuel mass per injection pulse can be assumed to be a linear function of the fuel injector on-time

$$m_{f,i} = g_i(T_i - T_{i,off}), \quad i = 1, \ldots, n_c,$$

where T_i is the time the injector is open (s), g_i the gain (kg/s) and $T_{i,off}$ the offset (s) of each injector. Therefore, the mean-value injected fuel mass flow is given by

$$\dot{m}_{f,i} = \frac{n}{30} g_i(T_i - T_{i,off}), \quad i = 1, \ldots, n_c. \tag{A.7}$$

In this relation the fuel flow dynamics, due to the wall wetting, can be neglected assuming the steady-state measurement condition. Moreover, the small dynamic coupling between the fuel subsystem and the air subsystem is ignored.

References

Aquino, C. F. (1981). *Transient A/F control characteristics of the 5 liter central fuel ignition engine*. Technical report No. 810494, SAE.

Balluchi, A., Benvenuti, L., Di Benedetto, M. D., Pinello, C., & Sangiovanni-Vincentelli, A. L. (2000). Automotive engine control and hybrid systems: Challenges and opportunities. *Proceedings of the IEEE*, Vol. 88, No. 7 (pp. 888–912).

Benvenuti, L., Di Benedetto, M. D., Rossi, C., & Sangiovanni-Vincentelli, A. (1998). Injector characteristics estimation for spark ignition engines. *Proceedings of the 37th IEEE conference on decision and control*, Tampa, FL (pp. 1546–1551).

Bush, K. J., Adams, N. J., Dua, S., & Markyvech, C. R. (1994). *Automatic control of cylinder by cylinder air–fuel mixture using a proportional exhaust gas sensor*. Technical report No. 940149, SAE.

Chang, C.-F., Fekete, N. P., Amstutz, A., & Powell, J. D. (1995). Air–fuel ratio control in spark-ignition engines using estimation theory. *IEEE Transactions on Control Systems Technology*, *3*(1), 22–31.

Chaumerliac, V., Bidan, P., & Boverie, S. (1994). Control-oriented spark ignition engine model. *Control Engineering Practice*, *2*(3), 381–387.

Choi, S. B., & Hedrick, J. K. (1998). An observer-based controller design method for improving air/fuel characteristics of spark ignition engines. *IEEE Transactions on Control Systems Technology*, *6*(3), 325–334.

Dobner, D. J. (1980). *A mathematical engine model for development of dynamic engine control*. Technical report No. 800054, SAE.

Fekete, N. P., Nester, U., Gruden, I., & Powell, J. D. (1995). *Model-based air–fuel ratio control of a lean multi-cylinder engine*. Technical report No. 950846, SAE.

Grizzle, J. W., Cook, J. A., & Milam, W. P. (1994). Improved cylinder air charge estimation for transient air–fuel ratio control. *Proceedings of the American control conference*, 1994, Vol. 2, 1568–1573.

Grizzle, J. W., Dobbins, K. L., & Cook, J. A. (1991). Individual cylinder air–fuel ratio control with a single EGO sensor. *IEEE Transactions on Vehicular Technology*, *40*(1), 280–286.

Hendricks, E., & Sorenson, S. C. (1990). *Mean value modelling of spark ignition engines.* Technical report No. 900616, SAE.

Hendricks, E., & Vesterholm, T. (1992). *The analysis of mean value SI engine models.* Technical report No. 920682, SAE.

Heywood, J. B. (1989). *Internal combustion engine fundamentals*. New York: McGraw-Hill Book Co., Inc.

Jones, V. K., Ault, B. A., Franklin, G. F., & Powell, J. D. (1995). Identification and air–fuel ratio control of a spark-ignition engine. *IEEE Transactions on Control Systems Technology*, *3*(1), 14–21.

Moraal, P. E., Cook, J. A., & Grizzle, J. W. (1993). Single sensor individual cylinder air–fuel ratio control of an eight cylinder engine with exhaust gas mixing. *Proceedings of the American control conference*, San Francisco, CA.

Powell, B. K., Wu, H., & Aquino, C. F. (1981). *Stoichiometric air–fuel ratio control analysis*. Technical report No. 810274, SAE.

Taylor, C. F., & Taylor, E. S. (1970). *The internal combustion engine* (2nd ed.). Scranton, PA: Int. Textbook Co.

Luca Benvenuti was born in Rome on February 8th, 1966. He received the Dottore in Ingegneria degree (Laurea) summa cum laude in Electrical Engineering from the University of Roma “La Sapienza”, in 1992. In 1995 he had been a visiting student at the Department of Electrical Engineering and Computer Science, University of California at Berkeley, in the research group of Professor S. Sastry. In 1996 he received the Ph.D. in System Engineering from the University of Rome, “La Sapienza” and in 1997–1999 he held a post-doc position at the University of L’Aquila. In 1997 he had consulted for Magneti Marelli and from 1997 to 2000 he was scientific consultant at the PARADES research laboratory in Rome. He is currently Assistant Professor at the Department of Computer and Systems Science (D.I.S.) of the University of Rome, “La Sapienza”. He is the co-recipient of the 2001 CAS Guillemin-Cauer Award for the best paper published in the IEEE Transactions on Circuits and Systems during the two calendar years preceding the award.

Maria Domenica Di Benedetto obtained the "Dr. Ing." degree (summa cum laude) of Electrical Engineering and Computer Science, University of Roma "La Sapienza" in 1976 (Mosè Ascoli Award). In 1981, she obtained the degree "Docteur-Ingénieur" and in 1987 the degree "Doctorat d'Etatès Sciences", Université de Paris-Sud, Orsay, France. From 1979 to 1983, she was research engineer at the scientific centers of IBM in Paris and Rome. From 1983 to 1987, she was "Ricercatore" at the University of Roma "La Sapienza". From 1987 to 1990, she was Associate Professor at the Istituto Universitario Navale of Naples. From 1990 to 1993, she was Associate Professor at the University of Roma "La Sapienza". Since 1994, she has been Professor of Control Theory at University of L'Aquila. From 1995 to 2002, she was Adjunct Professor, Department of EECS, University of California at Berkeley. In 1987, she was Visiting Scientist at MIT; in 1988, 1989 and 1992, Visiting Professor at the University of Michigan, Ann Arbor; in 1992, Chercheur Associé, C.N.R.S., Poste Rouge, Ecole Nationale Supérieure de Mécanique, Nantes, France; in 1990, 1992, 1994 and 1995, McKay Professor at the University of California at Berkeley. Her research interests revolve around nonlinear control and hybrid systems. She was Associate Editor of the IEEE Transactions of Automatic Control and has been Subject Editor of the International Journal of Robust and Nonlinear Control. She is the PI and Director of the Center of Excellence for Research DEWS on "Architectures and Design methodologies for Embedded controllers, Wireless interconnect and System-on-chip", University of L'Aquila. She is a Fellow of the IEEE.

Stefano Di Gennaro obtained the degree in Nuclear Engineering in 1987 (summa cum laude), and the Ph.D. in System Engineering in 1992, both from the University of Rome "La Sapienza", Rome, Italy. In October 1990 he joined the Department of Electrical Engineering, University of L'Aquila, as Assistant Professor of Automatic Control. Since 2002, he has been Associate Professor of Automatic Control at the University of L'Aquila. He holds courses on Automatic Control and Nonlinear Control. In 1986 he was visiting scientist, at the Nuclear Research Center "ENEA-Casaccia". From 1991 to 1998 he was visiting professor at the Laboratoire des Signaux et Systèmes, CNRS-Paris, and of the Department of Electrical Engineering of the Princeton University, New Jersey, USA, from 1993 to 1995. From 1993 to the present he has been visiting professor of the Centro de Investigacion y Estudios Avanzados del IPN, Unidad Ciudad de Mexico and Unidad Guadalajara, Mexico. In 1998 he visited the Department of Electrical Engineering and Computer Science, University of California at Berkeley, USA. He is working in the area of nonlinear control applied to spacecraft attitude control, electric machines, nonlinear regulation, and in the area of control of hybrid systems.

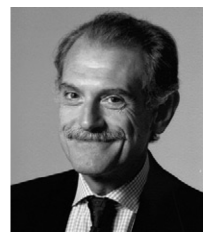

Alberto Sangiovanni Vincentelli is Professor of Electrical Engineering and Computer Sciences at the University of California at Berkeley where he has been on the Faculty since 1976. He is a co-founder of Cadence and Synopsys, the two leading companies in the area of Electronic Design Automation. He is the Chief Technology Advisor of Cadence and sits on the Board of Directors of Cadence. He also sits on the boards of Sonics, Accent and Softface. He is a member of the HP Strategic Technology Advisory Board. He has consulted for a number of companies including IBM, Intel, ATT, GTE, GE, Harris, Nynex, DEC, HP, Kawasaki Steel, Fujitsu, Sony, Hitachi, ST, Alcatel, BMW, Daimler-Chrysler, Magneti-Marelli, Bull. He is the Scientific Director of PARADES, a European Group of Economic Interest funded in 1996 by Cadence, Magneti-Marelli, and ST. In 1981 he received the Distinguished Teaching Award of the University of California and in 1995 the worldwide Graduate Teaching Award of the IEEE (a Technical Field award for "inspirational teaching of graduate students"). He has received three Best Paper Awards (1982, 1983 and 1990) and a Best Presentation Award (1982) at the Design Automation Conference, three best paper awards from the International VLSI conference, and is the co-recipient of the Guillemin-Cauer Award (1982–1983), the Darlington Award (1987–1988), and the Best Paper Award of the Circuits and Systems Society of the IEEE (1989–1990). He was the recipient of the 2001 EDA Kaufman Award and of the 2002 Aristotle Award of the SRC. He is the author of over 600 papers and fifteen books in the area of design methodologies and tools. Dr. Sangiovanni-Vincentelli has been a fellow of the Institute of Electrical and Electronics Engineers since 1982 and a Member of the National Academy of Engineering.